U Karst
Volume 08 Number 01 Year 2024

ISSN (*Online*) 2581-2157
ISSN (*Print*) 2502-9304

Available Online at
https://ojs.unik-kediri.ac.id/index.php/ukarst/index

https://dx.doi.org/10.30737/ukarst.v8i1.5485

U KaRsT

Abrams' Law Formulation for Blended Cement Paste Incorporated with Ground Ferronickel Slag

H. S. Djayaprabha[1*], A. H. Fatharani[2]

[1*,2] *Department of Civil Engineering, Engineering Faculty, Parahyangan Catholic University, Bandung, Indonesia*

Email: [1*] herry.suryadi@unpar.ac.id, [2] ashilahsy@gmail.com

A R T I C L E I N F O

Article History :
Article entry : 13 – 02 – 2024
Article revised : 04 – 03 – 2024
Article received : 15 – 04 – 2024

Keywords :
Abrams' Law, Blended Cement Paste, Compressive Strength, Ground Ferronickel Slag.

IEEE Style in citing this article:
H. S. Djayaprabha, and A. H. Fatharani, "Abrams' Law Formulation for Blended Cement Paste Incorporated with Ground Ferronickel Slag," U Karst, vol. 8, no. 1, pp 1 – 14, 2023, doi: 10.30737/ukarst.v8i1.5485.

A B S T R A C T

Ground ferronickel slag (GFS) is a form of an industrial waste by-product generated during the smelting process of nickel ore that has been crushed and ground into fine powder. GFS is a pozzolanic substance that may be employed as an environmentally beneficial binding agent when blended with Portland cement. This research aims to apply the Abrams Law formulation to blended cement combined with GFS. GFS was utilized as a Portland cement composite (PCC) replacement at varying percentages of 0, 10, 20, 30, 40, and 50 wt.%. The blended cement paste incorporated with GFS was tested at three water to cementitious material ratio (w/cm) levels of 0.4, 0.5, and 0.6. After samples have been made, a compressive strength test is carried out. The research results showed that at 28 days, the optimum amount of GFS was found in the percentage of 20 wt.% induced the compressive strength by 40.41 MPa with a w/cm of 0.4. The equations based on Abrams' Law have been proposed for estimating the correlation of 28-day compressive strength with w/cm in the range from 0.4 to 0.6. In addition, the hardened densities of binary blended cement paste were investigated. It was found that the density decreased with an increase of w/cm. The proposed equations provide the beneficial interpretation for estimating the compressive strength of blended cement paste based on the w/cm.

1. Introduction

Portland cement is a prominent hydraulic cement that can react with water to form cement paste as the aggregate binding agent in mortar and concrete. The production of Portland cement requires intensive energy consumption, and currently, it is responsible for almost 6-7% of the worldwide carbon dioxide (CO_2) discharge [1]. Concerning environmental impact, cement industries have started to produce the Portland cement composite (PCC) as the major hydraulic binder component for construction materials to reduce CO_2 emissions. Compared

ISSN (*Online*) 2581-2157
ISSN (*Print*) 2502-9304

with ordinary Portland cement (OPC) production, CO_2 emissions could be reduced by about 0.1-0.2 kg for every kg of PCC produced [2]. PCC is a commercial blended cement that contains both grounded cement clinker and gypsum together with one or more other inorganic substances, e.g., ground granulated blast furnace slag, pozzolan, limestone, etc., in a total content of 6% to 35% of the total mass of PCC [3].

As the world's most prominent supplier of nickel in the form of lateritic, Indonesia is ranked 6th in the world nickel reserves, with about 5% of the total world reserves [4]. Nickel ores are utilized in ferronickel production to manufacture nickel alloy and stainless steel [5], where during the smelting process of nickel ore and other compounds, the residue in the form of molten slag is discharged from the furnace. At temperatures of about 1500 °C, the molten slag is then rapidly cooled by a high-pressure water jet to disperse it into granular slag can be generated [6]. In the manufacturing process of 1 ton of ferronickel, there are about 14 tons of ferronickel slag [7]. Environmental pollution arises when huge amounts of ferronickel slag are not utilized and just dumped into the land with a huge area or valley [8]. On the other hand, the Indonesian government classified slag as hazardous waste by following Basel's Convention regulation [9], so it is a potential challenge for taking advantage of ferronickel slag as a useful waste material. In the construction materials area, this problem may be resolved by directly utilizing the granular ferronickel slag as both fine and coarse aggregates [10-13] or transferring granular ferronickel slag into ground ferronickel slag (GFS) powder. GFS powder, as one of the industrial waste by-products, showed pozzolanic properties with chemical compositions of GFS mainly including quicklime (CaO), magnesia (MgO), alumina (Al_2O_3), silica (SiO_2), and iron (III) oxide (Fe_2O_3) [14-16]. On the other hand, GFS also had a potential to be utilized in soft soil stabilization [17] and soil improvement [18].

Materials that have pozzolanic properties are often classified as supplementary cementitious materials (SCM). SCM is often utilized as a cement replacement, generally called blended cement [19]. The frequently utilized SCMs in construction materials are fly ash, ground granulated blast furnace slag, silica fume, limestone, and ground ferronickel slag, etc.[19; 20]. Utilization SCM has led researchers to find greener cement by mixing it directly to cement in binary, ternary, or quaternary systems [19; 21; 22] for producing aggregate binding agents. Therefore, the utilization of GFS powder as a binder has become a long-term strategy for reducing CO_2 emissions due to the use of less clinker cement [23; 24].

In concrete production, the water-to-cement ratio has an essential role in determining both fresh and hardened properties, including the workability, strength, and quality of the

https://dx.doi.org/10.30737/ukarst .v8i1.5485

ISSN (*Online*) 2581-2157
ISSN (*Print*) 2502-9304

concrete. The quantity of water in the paste portion impacts the strength of hardened paste that controls the strength of structural concrete, and lesser water content in cement leads to greater strength [25]. Therefore, the compressive strength prediction based on the water amount for the specified cement type is important for being determined. The correlation between compressive strength and water content in concrete, previously proposed by Duff Abram in 1918 [26], indicates that the ratio of water content to cement content has an inverse correlation with compressive strength. The correlation, popularly known as Abrams' Law, is useful for estimating the compressive strength of cementitious materials depending on their w/c. Abrams' Law typically only defines a specific relationship for Portland cement concrete. Previous research explored the effect of a water-to-cement ratio from 0.5 to 1.2 on cement mortar with five different cement-to-sand ratios, with results showed that the Abrams' Law formulation is still applicable for cement mortars with different proportions [27]. Another study found that the Abrams' Law formulation is applicable for cement-based mortar with a water-to-cement ratio greater than 0.40 [28]. From those previous studies, it could be seen that most of the Abrams' Law formulation is applicable to cement-based materials and there is currently insufficient study into the formulation for blended cement containing GFS.

The principal objective of the current experimental investigation is to seek the possibilities of the application of Abrams' Law formulation in terms of the correlation between compressive strength and w/cm in blended cement incorporated with GFS at a replacement level from 0 to 50 wt.%. The findings of this research could potentially be regarded as a substantial addition for estimating compressive strength in concrete produced using PCC incorporated with GFS.

2. Research Method

In performing this experimental research, the locally sourced materials were prepared, and their material properties were investigated. The mixture proportions were calculated by using the absolute volume method. Compressive strength tests were performed at specified ages to determine the optimal amount of GFS replacement and to establish Abrams' Law formulation for blended cement paste. The comprehensive research methods were outlined in the following subsections.

2.1 PCC and GFS

The PCC sourced from Indonesia, which meets the Indonesian National Standards SNI 15-7064-2004 [3] and has a specific gravity of 2.93, was utilized. The grayish GFS powder was

https://dx.doi.org/10.30737/ukarst .v8i1.5485

ISSN (*Online*) 2581-2157
ISSN (*Print*) 2502-9304

obtained from PT Growth Java Industry with a specific gravity of 2.76, as shown in **Figure 1**. ASTM C188 [29] was used to determine the densities of both powders using the Le Chatelier flask method. The chemical compositions of the GFS used in this study can be found in **Table 1**. **Figure 2** demonstrated the GFS mineralogical phases that were explored with an X-Ray diffractometer (XRD). From the XRD test, it could be revealed that the GFS exhibited the amorphous phase with a hump in 2θ approximately between 25° and 35°.

Source: Authors Documentation

Figure 1. Physical Appearance of GFS

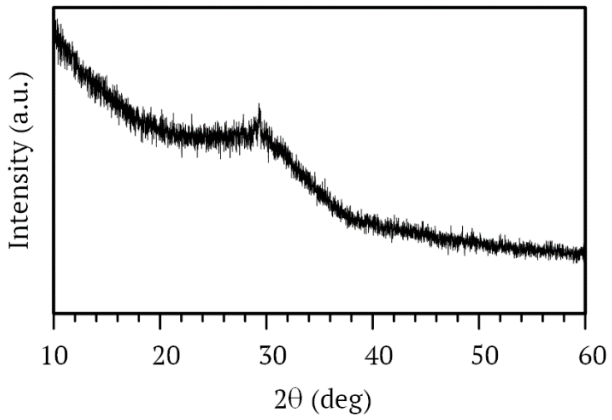

Source: Authors Documentation

Figure 2. XRD Pattern of GFS.

Table 1. Chemical Compositions of GFS.

Parameters	Value (%)	Parameters	Value (%)
Ni	0.09	SiO_2	40.69
CO	0.02	P_2O_5	0.21
Fe	2.24	SO_3	0.37
Fe_2O_3	3.20	K_2O	0.24
CaO	24.83	TiO_2	0.19
MgO	18.81	Cr	0.68
Na_2O	0.44	Cr_2O_3	0.99
Al_2O_3	6.23	MnO	0.68
		Lost on Ignition	1.25

Source: Kuncoro and Djayaprabha, (2021) [14].

https://dx.doi.org/10.30737/ukarst .v8i1.5485

ISSN (*Online*) 2581-2157
ISSN (*Print*) 2502-9304

2.2 Mixture Proportions

Both PCC and GFS powder were utilized for making binary blended cement by replacing PCC partially with GFS powder at varied weight ratios (α) from 0 to 50 wt.% of total cementitious materials mass, which can be calculated with Equation (1):

$$\alpha = \frac{W_{GFS}}{W_{PCC} + W_{GFS}} \quad (1)$$

where W_{PCC} is the weight of PCC (kg/m^3) and W_{GFS} is the weight of GFS powder (kg/m^3).

The summary of mixture proportions of binary blended cement paste incorporating GFS at replacement ratios of 0, 10, 20, 30, 40, and 50 wt.%. Three different w/cm ratios of 0.4, 0.5, and 0.6, calculated on an absolute volume basis with water content variation, were presented in **Table 2**. The first number in the mixture code represented the w/cm, while the code after the dashed line represented the proportion of GFS used to replace PCC.

Table 2. Binary Blended Cement Paste Mixture Proportions.

Code	*w/cm*	PCC (wt.%)	GFS (wt.%)	Water (kg/m^3)	PCC (kg/m^3)	GFS (kg/m^3)
0.4-GFS0	0.4	100	0	550	1350	0
0.4-GFS10		90	10	538	1211	135
0.4-GFS20		80	20	537	1074	268
0.4-GFS30		70	30	535	937	401
0.4-GFS40		60	40	534	801	534
0.4-GFS50		50	50	532	665	665
0.5-GFS0	0.5	100	0	595	1189	0
0.5-GFS10		90	10	593	1068	119
0.5-GFS20		80	20	592	946	237
0.5-GFS30		70	30	590	826	354
0.5-GFS40		60	40	589	706	471
0.5-GFS50		50	50	587	587	587
0.6-GFS0	0.6	100	0	638	1063	0
0.6-GFS10		90	10	636	954	106
0.6-GFS20		80	20	635	846	212
0.6-GFS30		70	30	633	739	317
0.6-GFS40		60	40	632	632	421
0.6-GFS50		50	50	630	525	525

Source: Authors Data

2.3 Specimen Preparation and Testing Method

The blended cement was obtained by mixing dry PCC and GFS powders in every proportion. The mixing sequence for producing binary blended cement paste followed ASTM C305 [30]. The blended cement was placed into the mixing bowl along with the mixing water. After allowing the cement 30 seconds to absorb the water, the paddle mixer was turned on for 30 seconds at a slow pace. After 15 seconds, turn off the mixer and scrape down any sticking paste on the edges of the mixing bowl, then run the mixer at medium speed for another 60 seconds. The cubic molds were filled with the fresh paste, and the air bubbles were reduced by

https://dx.doi.org/10.30737/ukarst .v8i1.5485

ISSN (*Online*) 2581-2157
H. S. Djayaprabha / U Karst Vol 08 No. 01 Year 2024 ISSN (*Print*) 2502-9304

manual tamping, adopting the ASTM C109/C109M [31] procedure. The compressive strength tests were determined using triplicate 50-mm cubic. The compressive strength of hardened cement paste (f_p) was determined by dividing the peak load at failure (P_{max}) with the average of loaded surface area (A) for each specimen [32], where the P_{max} was determined by conducting a compression test on a 50-mm cubic specimen using a compressive testing machine.

Before conducting the tests, the actual specimen's dimensions of the 50-mm cubic were measured using a digital caliper and its actual volume (V) was calculated. Furthermore, the specimen's mass (m) was measured with a 0.01 g digital scale. Then, the density of hardened binary blended cement paste (ρ_{bcp}) was calculated by dividing m with V.

2.4 Abrams' Law Formulation

Abram developed the equation for modeling the increment of compressive strength as the w/c decreased. The equation is regarded as a significant contribution in the history of concrete technology. The Abrams' Law formulation could be widely utilized for estimating the compressive strength of concrete (f_c) as a function of w⁄c as water-to-cement ratio and A and B as empirical constants acquired through fitted curves to experimental data as shown in Equation (2) [33].

$$f_c = \frac{A}{B^{w/c}} \tag{2}$$

3. Results and Discussions

3.1 Compressive Strength of Blended Cement Paste

The effect of GFS powder at replacement ratios of 0, 10, 20, 30, 40, and 50 wt.% on the compressive strength of hardened blended cement paste in three different w/cm ratios of 0.4, 0.5, and 0.6 were examined. The development of compressive strength from 7 to 56 days for each level could be investigated in **Figure 3** for w/cm ratios equal to 0.4, 0.5, and 0.6, respectively. Because the early reaction degree of GFS powder is slower when compared to pure PCC paste, the early compressive strength of the blended cement pastes was lower than that of PCC paste for entire w/cm ratios [34]. However, after 28 days of curing, the compressive strength of the blended cement paste was higher than that of the PCC-based cement paste. The formation of calcium silicate hydrate (CSH) gel, which contributes more strength, is the result of a pozzolanic reaction that increased the number of hydration products. This reaction involved combining amorphous silica from GFS with portlandite from the hydration of calcium silicate phases in PCC [19].

https://dx.doi.org/10.30737/ukarst .v8i1.5485

U Karst
Volume 08 Number 01 Year 2024
ISSN (*Online*) 2581-2157
ISSN (*Print*) 2502-9304

As shown in **Figure 3(a)**, the pure PCC paste with a w/cm of 0.4 had a 28-day compressive strength (f_{p28}) of 38.33 MPa. When comparing with that of the pure PCC paste, f_{p28} with the same w/cm at replacement ratios of 10%, 20%, 30%, 40%, and 50% were 1.23% higher (38.80 MPa), 5.44% higher (40.41 MPa), 0.98% lower (37.95 MPa), 4.75% lower (36.51 MPa), and 15.75% lower (32.29 MPa), respectively. Essentially, the hydration reaction of cementitious materials was scarcely completed after 28 days, and creating more CSH gels triggered long-term strength development [35]. The compressive strength of the mixes with a w/cm of 0.4 and replacement ratios of 10, 20, 30, 40, and 50 wt.% was increased by 10.56%, 14.28%, 27.06%, 23.18%, 21.81%, and 35.85% after 56 days in comparison to the f_{p28}. These results are in line with previous research, which mentioned that the long-term compressive strength of GFS blended mixtures had a pozzolanic reaction that was similar to that of concrete containing pozzolanic material such as fly ash [36]. On the other hand, the rise in w/cm caused the compressive strength to significantly drop for all replacement ratios. At a replacement ratio of 20%, the f_{p28} of mixtures with w/cm of 0.5 and 0.6 are lower by 37.36% and 58.69% when compared with the mixture with w/cm of 0.4. This phenomenon happens due to the rise in w/cm, less of the paste's volume is involved in the process of nucleation and growth of CSH [37].

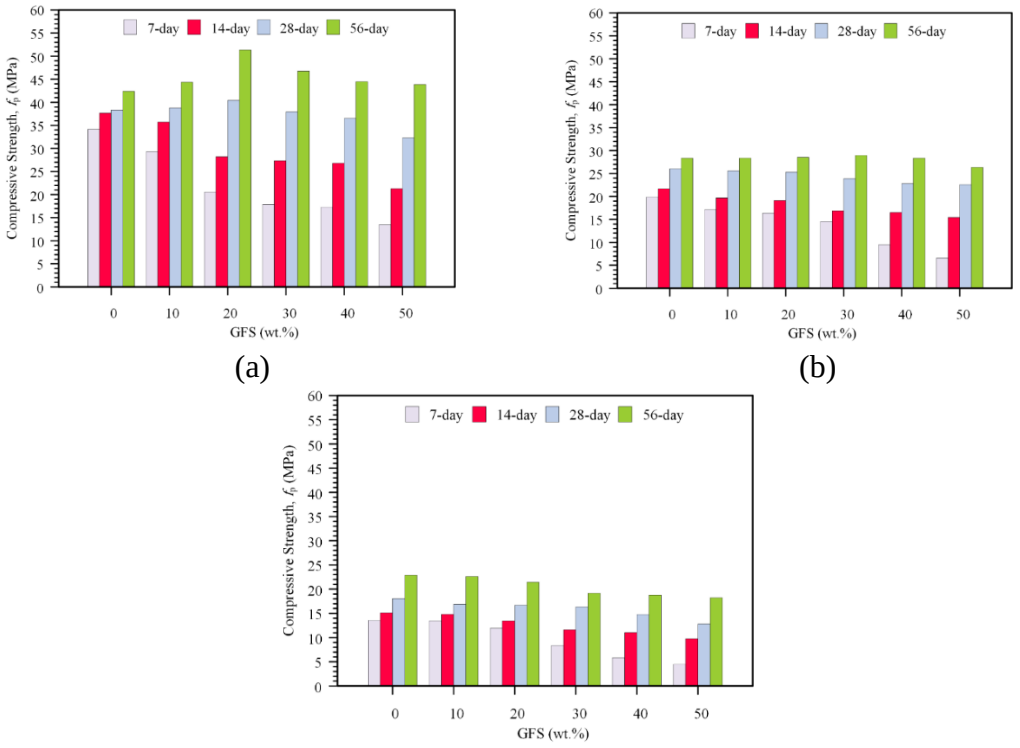

Source: Authors Data

Figure 3. The f_p of Blended Cement Paste with the GFS variation in (a) *w/cm* = 0.4, (b) *w/cm* = 0.5, and *w/cm* = 0.6.

https://dx.doi.org/10.30737/ukarst .v8i1.5485

ISSN (*Online*) 2581-2157
ISSN (*Print*) 2502-9304

3.2 Hardened Density of Binary Blended Cement Paste

The hardened densities of binary blended cement paste specimens with three different ratios of w/cm of 0.4, 0.5, and 0.6 were investigated at 28 days, as shown in **Table 3**. The density of hardened cement paste could be altered by several factors, such as cement type, w/cm, utilization of SCM, etc. Based on the results (**Table 3**), it could be seen that the higher replacement ratio of GFS induced lower density of the cement paste due to the specific gravity of GFS in the value of 2.76, which is slightly lower than that of PCC in the value of 2.93. A similar trend of decreasing hardened density as increasing of GFS content in blended mixtures was also found by Bouasria et al. in 2022 [38]. Furthermore, it was also discovered that the greater the w/cm, the lower the hardened density of binary blended cement paste, due to the capillary porosity of cement paste increasing in the higher water to cement ratio [39].

Table 3. Hardened Density of Blended Cement Paste.

w/cm	ρ_{bcp} (kg/m^3)					
	GFS0	**GFS10**	**GFS20**	**GFS30**	**GFS40**	**GFS50**
0.4	1868.91	1860.11	1867.58	1851.20	1841.19	1854.98
0.5	1754.66	1730.05	1719.00	1726.18	1751.62	1730.33
0.6	1735.49	1715.93	1710.98	1704.17	1686.78	1686.75

Source: Authors Data.

3.3 Abrams' Law Formulation of Blended Cement Paste

The general Abrams' Law formulation was adopted to determine the compressive strength of hardened blended cement paste incorporated with GFS at 28 days (f_{p28}) as a function of A, B, and w/cm. In this study, the w/cm was taken at three levels of 0.4, 0.5, and 0.6 due to Abrams' Law being effective when w/cm is over a range of 0.3 to 1.20 [40; 41]. From the test results that can be investigated in **Figure 4**, it could be concluded that the trend of f_p follows the general trend of Abrams' Law. Therefore, it is feasible to use Abrams' Law for formulating the correlation between f_p and w/cm. The best-fit curve was determined, and equations were proposed to describe the correlation of f_{p28} and w/cm at replacement ratios of 0, 10, 20, 30, 40, and 50 wt.%. The results were demonstrated in **Figures 4(a)** to **4(f)**. The empirical constants of A and B were obtained by using a solver in a spreadsheet for solving the non-linear equation. Those empirical constants could be used to develop and estimate the role of w/cm in the compressive strength development.

https://dx.doi.org/10.30737/ukarst .v8i1.5485

ISSN (*Online*) 2581-2157
ISSN (*Print*) 2502-9304

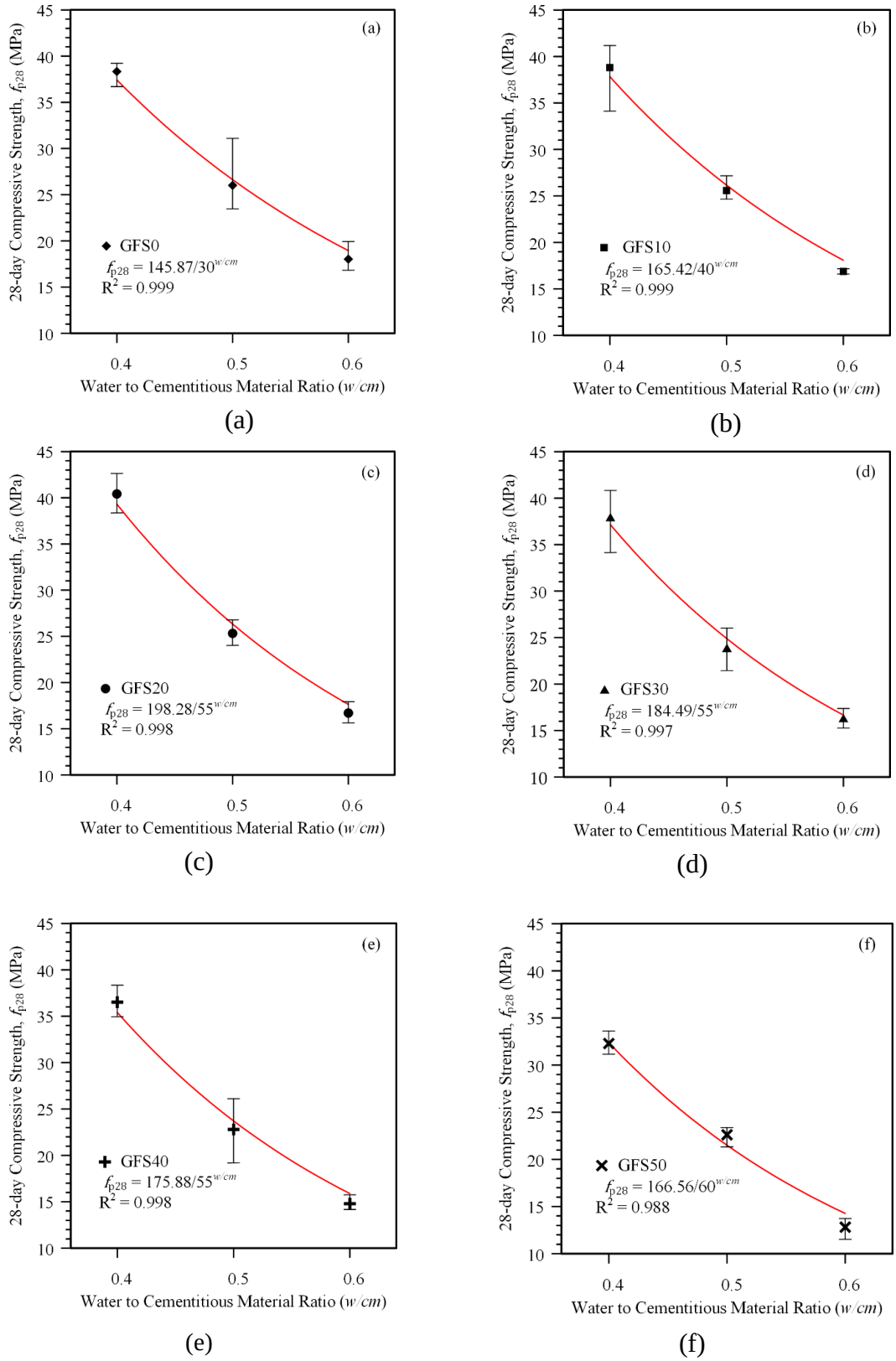

Source: Authors Data.

Figure 4. Abrams' Law formulation of (a) GFS0; (b) GFS10; (c) GFS20; (d) GFS30; (e) GFS40; (f) GFS50.

https://dx.doi.org/10.30737/ukarst .v8i1.5485

10 - 14
ISSN (*Online*) 2581-2157
ISSN (*Print*) 2502-9304

The summary of the empirical constants based on Abrams' law that were obtained from the best-fit curve to the experimental data can be found in **Table 4**. The coefficient of determination (R^2) for the proposed equations was above 0.98, indicating a high correlation between the f_p and w/cm at 28 days, and the proposed equations could be considered highly accurate for estimating concrete compressive strength.

Table 4. Empirical Constants and Coefficient of Determination of Proposed Equations.

Code	*A*	*B*	R^2
GFS0	145.87	30	0.999
GFS10	165.42	40	0.999
GFS20	198.28	55	0.998
GFS30	184.49	55	0.997
GFS40	175.88	55	0.998
GFS50	166.56	60	0.988

Source: Authors Data.

Some researchers have also proposed adjustments of the Abrams' Law formulation for construction materials that incorporate pozzolanic materials. Mondal and Bhanja in 2022 used statistical methods to create a model that considers some factors that influence the compressive strength of fly ash concrete [42]. A modification of Abrams' Law also carried out by ElNemr in 2020 using regression analysis for estimating the compressive strength of mortar incorporating 15% silica fume for use in masonry walls [43]. In the current study, the proposed equations are still limited to the specified number of GFS in the blended cement. Therefore, the modification of Abrams' Law with the addition of parameters for estimating the GFS content should be considered for the research extension.

4. Conclusions

The influence of the water to cementitious ratio of a binary blended composite cement binder from Portland cement composite and ground ferronickel slag has been successfully developed. The study discovered that employing ground ferronickel slag at amount of 20 wt.% at a w/cm of 0.4 might be beneficial with an optimal compressive strength of 40.41 MPa at 28 days and 51.36 MPa at 56 days. There is a substantial connection between compressive strength and water to cementitious ratio, which suggests that the mathematical formulation of Abrams' Law is still an acceptable choice for evaluating this relationship. Which is supported by the

https://dx.doi.org/10.30737/ukarst .v8i1.5485

ISSN (*Online*) 2581-2157
ISSN (*Print*) 2502-9304

strong correlation between the two variables with R^2 greater than 0.98. The proposed equations that were obtained in this study could be used as a reference for the interpreting 28-day compressive strength of blended cement paste with replacement ratios of 0, 10, 20, 30, 40, and 50 wt.% a with variation of water to cementitious material ratio.

5. Acknowledgements

The authors are thankful for the contribution from PT Growth Java Industry through agreement No. III/FT-Spl/2019-04/178-MOU in supplying GFS and Structural Engineering Laboratory UNPAR for providing the experimental facilities.

https://dx.doi.org/10.30737/ukarst .v8i1.5485

12 - 14
ISSN (*Online*) 2581-2157
ISSN (*Print*) 2502-9304

References

[1] Global Efficiency Intelligence, "*Global Cement Industry's GHG Emissions*", Available: https://www.globalefficiencyintel.com/new-blog/2021/global-cement-industry-ghg-emissions, Accessed: 16 December 2023.

[2] Asosiasi Semen Indonesia, "*Upaya Industri Semen dalam Pengendalian Emisi Gas Rumah Kaca*", Available: https://asi.or.id/upaya-industri-semen-dalam-pengendalian-emisi-gas-rumah-kaca/, Accessed: 16 December 2023.

[3] SNI 15-7064-2004, *Semen Portland Komposit*, Jakarta, Badan Standardisasi Nasional, 2004.

[4] Ferhi, D. A., Cahyaningsih, S. and Pujilestari, E. (2019). Inovasi dan Efisiensi Limbah Slag Nikel yang Bernilai Tambah. Jakarta, PT Antam Tbk.

[5] Luo, Z., Ma, Y., Mu, W., Liu, J., He, J. and Zhou, X., "Magnesium Phosphate Cement Prepared with Electric Furnace Ferronickel Slag: Properties and Its Hydration Mechanism," *Constr. Build. Mater.*, vol. 300, 123991, 2021, doi:10.1016/j.conbuildmat.2021.123991.

[6] Hui, W., Suping, C. and Yali, W., "Influence of Cooling Ways on the Structure and Hydraulic Activity of Blast Furnace Slag," *Key Eng. Mater.*, vol. 633, pp. 234-239, 2015, doi:10.4028/www.scientific.net/KEM.633.234.

[7] Saha, A. K. and Sarker, P. K., "Expansion due to Alkali-silica Reaction of Ferronickel Slag Fine Aggregate in OPC and Blended Cement Mortars," *Constr. Build. Mater.*, vol. 123, pp. 135-142, 2016, doi:10.1016/j.conbuildmat.2016.06.144.

[8] Nuruzzaman, M., Casimiro, J. O. C. and Sarker, P. K., "Fresh and Hardened Properties of High Strength Self-compacting Concrete using by-product Ferronickel Slag Fine Aggregate," *J. Build. Eng.*, vol. 32, 101686, 2020, doi:10.1016/j.jobe.2020.101686.

[9] Zulhan, Z. and Agustina, N., "A Novel Utilization of Ferronickel Slag as a Source of Magnesium Metal and Ferroalloy Production," *J. Clean. Prod.*, vol. 292, 125307, 2021, doi:10.1016/j.jclepro.2020.125307.

[10] Sun, J., Feng, J. and Chen, Z., "Effect of Ferronickel Slag as Fine Aggregate on Properties of Concrete," *Constr. Build. Mater.*, vol. 206, pp. 201-209, 2019, doi:10.1016/j.conbuildmat.2019.01.187.

[11] Petrounias, P., Rogkala, A., Giannakopoulou, P. P., Christogerou, A., Lampropoulou, P., Liogris, S., Koutsovitis, P. and Koukouzas, N., "Utilization of Industrial Ferronickel Slags as Recycled Concrete Aggregates," *Applied Sciences*, vol. 12, no. 4, 2231, 2022, doi:10.3390/app12042231.

[12] Han, F., Zhang, H., Li, Y. and Zhang, Z., "Recycling and comprehensive utilization of ferronickel slag in concrete," *J. Clean. Prod.*, vol. 414, 137633, 2023, doi:10.1016/j.jclepro.2023.137633.

[13] Bao, J., Yu, Z., Wang, L., Zhang, P., Wan, X., Gao, S. and Zhao, T., "Application of ferronickel slag as fine aggregate in recycled aggregate concrete and the effects on transport properties," *J. Clean. Prod.*, vol. 304, 127149, 2021, doi:10.1016/j.jclepro.2021.127149.

[14] Kuncoro, A. and Djayaprabha, H. S., "The Effect of Sodium Hydroxide Molarity on the Compressive and Splitting Tensile Strength of Ferronickel Slag-Based Alkali Activated Mortar," *Media Komunikasi Teknik Sipil*, vol. 27, no. 2, pp. 151-160, 2021, doi:10.14710/mkts.v27i2.32706.

[15] Yang, T., Yao, X. and Zhang, Z., "Geopolymer Prepared with High-magnesium Nickel Slag: Characterization of Properties and Microstructure," *Constr. Build. Mater.*, vol. 59, pp. 188-194, 2014, doi:10.1016/j.conbuildmat.2014.01.038.

ISSN (*Online*) 2581-2157
ISSN (*Print*) 2502-9304

[16] Edwin, R. S., Kimsan, M., Tamburaka, I. P., Pramono, B., Azis, A., Heede, P. V. d., Belie, N. D. and Gruyaert, E., "Effect of Ferronickel Slag as Cementitious Material on Strength of Mortar " *Key Eng. Mater.*, vol. 931, pp. 213-218, 2022, doi:10.4028/p-n4v7se.

[17] Lim, A. and Darian, E., "Perbaikan Tanah Lunak Menggunakan Campuran Ferronickle Slag dan Kalium Serta Natrium Hidroksida," *Jurnal Rekayasa Sipil*, vol. 18, no. 3, 202-213, 2022, doi:10.25077/jrs.18.3.202-213.2022.

[18] Lim, A., Renaldy, A. and Kristian, D., "Soil Improvement of Petobo Silty Sand using Ferronickel Slag and Alkaline Activators," *ARCEE*, vol. 4, no. 2, 73-83, 2023, doi:10.32722/arcee.v4i02.5714.

[19] Lemonis, N., Tsakiridis, P. E., Katsiotis, N. S., Antiohos, S., Papageorgiou, D., Katsiotis, M. S. and Beazi-Katsioti, M., "Hydration Study of Ternary Blended Cements Containing Ferronickel Slag and Natural Pozzolan," *Constr. Build. Mater.*, vol. 81, pp. 130-139, 2015, doi:10.1016/j.conbuildmat.2015.02.046.

[20] Kosmatka, S. H. and Wilson, M. L. (2011). Design and Control of Concrete Mixtures 15th Edition. Skokie, Portland Cement Association.

[21] Radwan, M. K. H., Onn, C. C., Mo, K. H., Yap, S. P., Ng, C. G. and Yusoff, S., "Eco-mechanical Performance of Binary and Ternary Cement Blends Containing Fly Ash and Slag," *Proceedings of the Institution of Civil Engineers - Engineering Sustainability*, vol. 174, no. 1, pp. 23-36, 2021, doi:10.1680/jensu.20.00009.

[22] Schöler, A., Lothenbach, B., Winnefeld, F. and Zajac, M., "Hydration of Quaternary Portland Cement Blends Containing Blast-furnace Slag, Siliceous Fly Ash and Limestone Powder," *Cem. Concr. Compos.*, vol. 55, pp. 374-382, 2015, doi:10.1016/j.cemconcomp.2014.10.001.

[23] Kuri, J. C., Khan, M. N. N. and Sarker, P. K., "Fresh and Hardened Properties of Geopolymer Binder using Ground High Magnesium Ferronickel Slag with Fly Ash," *Constr. Build. Mater.*, vol. 272, 121877, 2021, doi:10.1016/j.conbuildmat.2020.121877.

[24] Kurniati, E. O., Pederson, F. and Kim, H.-J., "Application of Steel Slags, Ferronickel Slags, and Copper Mining Waste as Construction Materials: A Review," *Resources, Conservation and Recycling*, vol. 198, 107175, 2023, doi:10.1016/j.resconrec.2023.107175.

[25] Popovics, S. and Ujhelyi, J., "Contribution to the Concrete Strength versus Water-Cement Ratio Relationship," *J. Mater. Civ. Eng.*, vol. 20, no. 7, pp. 459-463, 2008, doi:10.1061/(ASCE)0899-1561(2008)20:7(459).

[26] Radhakrishna, "Strength Assessment in Portland Cement and Geopolymer Composites with Abrams' Law as Basis," *J. Adv. Concr. Technol.*, vol. 18, no. 6, pp. 320-327, 2020, doi:10.3151/jact.18.320.

[27] Singh, S. B., Munjal, P. and Thammishetti, N., "Role of Water/cement Ratio on Strength Development of Cement Mortar," *J. Build. Eng.*, vol. 4, pp. 94-100, 2015, doi:10.1016/j.jobe.2015.09.003.

[28] Rao, G. A., "Generalization of Abrams' law for cement mortars," *Cem. Concr. Res.*, vol. 31, pp. 495-502, 2001, doi:10.1016/S0008-8846(00)00473-7.

[29] ASTM C188-16, *Standard Test Method for Density of Hydraulic Cement*, West Conshohocken, ASTM International, 2016.

[30] ASTM C305-14, *Standard Practice for Mechanical Mixing of Hydraulic Cement Pastes and Mortars of Plastic Consistency*, West Conshohocken, ASTM International, 2014.

[31] ASTM C109-16, *Standard Test Method for Compressive Strength of Hydraulic Cement Mortars (Using 2-in. or [50-mm] Cube Specimens)*, West Conshohocken, ASTM International, 2016.

ISSN (*Online*) 2581-2157
ISSN (*Print*) 2502-9304

[32] Widodo, S., Ma'arif, F., Nugroho, M. S. and Mahardika, H., "Correlation of Ultrasonic Pulse Velocity with Porosity and Compressive Strength of Mortar with Limestonefor Building Quality Assessment," *U Karst*, vol. 6, no. 2, pp. 191-202, 2022, doi:10.30737/ukarst.v6i2.3508.

[33] Kargari, A., Eskandari-Naddaf, H. and Kazemi, R., "Effect of cement strength class on the generalization of Abrams' law," *Struct. Concr.*, vol. 20, no. 1, pp. 493-505, 2018, doi:10.1002/suco.201700275.

[34] Huang, Y., Wang, Q. and Shi, M., "Characteristics and Reactivity of Ferronickel Slag Powder," *Constr. Build. Mater.*, vol. 156, pp. 773–789, 2017, doi:10.1016/j.conbuildmat.2017.09.038.

[35] Djayaprabha, H. S., Chang, T.-P. and Shih, J.-Y., "Long-term Mechanical Properties of No-cement Slag Based Cementitious Binder Activated with Calcined Dolomite," *The 8th International Conference of Asian Concrete Federation*, pp. 75-80, 2018.

[36] Rahman, M. A., Sarker, P. K., Shaikh, F. U. A. and Saha, A. K., "Soundness and Compressive Strength of Portland Cement Blended with Ground Granulated Ferronickel Slag," *Constr. Build. Mater.*, vol. 140, pp. 194-202, 2017, doi:10.1016/j.conbuildmat.2017.02.023.

[37] Ley-Hernandez, A. M., Lapeyre, J., Cook, R., Kumar, A. and Feys, D., "Elucidating the Effect of Water-To-Cement Ratio on the Hydration Mechanisms of Cement," *ACS Omega*, vol. 3, pp. 5092-5105, 2018, doi:10.1021/acsomega.8b00097.

[38] Bouasria, M., Babouri, L., Khadraoui, F., Chateigner, D., Gascoin, S., Pralong, V., Benzaama, M.-H., Orberger, B. and Mendili, Y. E., "Insight Into the Partial Replacement of Cement by Ferronickel Slags from New Caledonia," *Eur. J. Environ. Civ. Eng.*, vol. 26, no. 8, pp. 3662-3680, 2022, doi:10.1080/19648189.2020.1814421.

[39] Bede, A. and Ardelean, I., "Revealing the influence of water-cement ratio on the pore size distribution in hydrated cement paste by using cyclohexane," *AIP Conference Proceedings*, vol. 1917, 040002, 2017, doi:10.1063/1.5018284.

[40] Sear, L. K. A., Dews, J., Kite, B., Harris, F. C. and Troy, J. F., "Abrams Law, Air and High Water-to-cement Ratios " *Constr. Build. Mater.*, vol. 10, no. 3, pp. 221-226, 1996, doi:10.1016/0950-0618(95)00079-8.

[41] Li, S., Yang, J. and Zhang, P., "Water-Cement-Density Ratio Law for the 28-Day Compressive Strength Prediction of Cement-Based Materials," *Adv. Mater. Sci. Eng.* , vol. 2022, 7302173 2022, doi:10.1155/2020/7302173.

[42] Mondal, A. and Bhanja, S., "Augmentation of Abrams Law for Fly Ash Concrete," *Mater. Today Proc.*, vol. 65, no. 2, pp. 644-650, 2022, doi:10.1016/j.matpr.2022.03.204.

[43] ElNemr, A., "Generating Water/binder Ratio to Strength Curves for Cement Mortar Used in Masnory Walls," *Constr. Build. Mater.*, vol. 233, 117249, 2020, doi:10.1016/j.conbuildmat.2019.117249.